

# EXPERIMENTAL STUDY OF THE THERMAL BEHAVIOUR OF HYDROGEN TANKS DURING HYDROGEN CYCLING

de Miguel, N.<sup>1</sup>, Acosta, B., Moretto, P., Harskamp, F. and Bonato, C.

<sup>1</sup> Institute for Energy and Transport, Joint Research Centre of the European Commission, P.O. Box 2, Petten, 1755ZG, The Netherlands, [nerea.de-miguel-echevarria@ec.europa.eu](mailto:nerea.de-miguel-echevarria@ec.europa.eu)

## ABSTRACT

The thermal behaviour of several commercial hydrogen tanks has been studied during high pressure (70-84 MPa) hydrogen cycling. The temperature of the gas at different points inside the tank, the temperature at the bosses and the tank outer wall temperature have been measured under different filling and emptying conditions. From the experimental results, the effect of the filling rate (1.4-9.2 g/s) and the influence of the liner material on the thermal behaviour of the hydrogen tanks have been evaluated. The thermal response of the metallic bosses under different cycling conditions has also been investigated.

*Keywords: hydrogen tanks, high pressure, hydrogen cycling, thermal behaviour, thermal response of the bosses.*

## 1. INTRODUCTION

Compared to fossil fuels and as an energy carrier, hydrogen has advantages with regard to availability and environmental impact, though several technical and economic problems require solution before industrial application, particularly with respect to production and storage [1].

In the particular case of transport, one of the principal issues is the storage of hydrogen inside the vehicle [2]. One of the current storage systems for hydrogen-powered vehicles is a compressed hydrogen storage tank. Due to the low density of hydrogen and in order to have vehicles with a similar autonomy to current (gasoline or diesel) ones, it should be stored at high pressures (up to more than 70 MPa) [2, 3].

Carbon fibre fully wrapped-reinforced tanks are already in use in hydrogen fuelled vehicles under demonstration. Two types of inner liners are typically used: metal (Al or Cr alloys) in Type III tanks and high molecular weight polymer for Type IV tanks. The application of such materials comes from the need of guaranteeing impermeability of the inner liner to the hydrogen molecules whilst being as lightweight as possible [4]. Type IV vessels are the most recently developed ones and their usage is gradually increasing because of characteristics such as low weight, durability and simple manufacturability. However, Type IV vessels have demerits related to problems such as plastic liner leaks and defects and the delamination between the plastic liner and the composite wrapping materials caused by temperature rise [5].

When an on-board hydrogen tank is refuelled, there are some technological limits, such as temperature, pressure, mass filling rate and the level of filling that should be considered. For safety reason, regulations and standards for hydrogen powered vehicles [6-8] require that in normal conditions, including filling and discharging, hydrogen temperature inside the tank shall not exceed 85 °C and not be less than -40 °C. The SAE J2601 standard of fuelling protocols for gaseous hydrogen vehicles [9] specifies that the maximum filling pressure, regardless of filling conditions or temperature, shall not be higher than 125% of the Nominal Working Pressure (NWP), a value which corresponds to 87.5 MPa for a tank with a NWP of 70 MPa. The NWP is defined as the container's service pressure as specified by the manufacturer at a uniform gas temperature of 15°C and full gas content.

During the fast, nearly adiabatic hydrogen filling process, the heat of compression and, to a much less extent, the Joule-Thomson effect, lead to a warming of the gas inside the tank [10]. The temperature

rise is a major challenge in the whole refuelling process. A too fast fill will result in exceeding the safety limit set on the maximal allowed temperature of the tank materials. On the other hand, practical and consumer' comfort considerations make unacceptable a duration of the refuelling longer than 3 - 5 minutes [11].

Once the refuelling is finished, the warm tank slowly cools down as heat is transferred to its cooler surroundings. The decreasing gas temperature is accompanied by a pressure decrease, and this decrease continues until the gas temperature is equal to the ambient temperature. The finally "settled" pressure is less than the pressure immediately after refuelling. If this pressure is less than the NWP, the tank will result under filled and the so-called State of Charge (SOC) will be less than the desired 100% [12]. According to the SAE J2601 standard [9] the SOC, which describes the grade of filling of the tank, is defined by the following equation:

$$SOC(\%) = \frac{\rho_{H_2}(P,T)}{\rho_{H_2}(NWP,15^{\circ}C)} \cdot 100, \quad (1)$$

where  $\rho_{H_2}$  represents the hydrogen density after filling which is a function of P (the pressure in the tank) and T (the temperature in the tank). The  $\rho_{H_2}$  at 70 MPa and 15°C is 40.2 g/L. After a filling, SOC should be as close to 100% as possible but not over it. Usually the final temperature at the end of the refuelling is higher than 15°C, so that the final target pressure should be higher than NWP to compensate for the pressure decrease caused by the post-filling cooling of the hydrogen.

Because of the technological importance of the refuelling process, many researchers have already studied the temperature behaviour of the hydrogen tanks during hydrogen filling [13-19]. It has been shown that the temperature rise in Type IV tanks (plastic liner) is higher than in Type III tanks (metallic liner). It has been also found that the temperature rise inside tank increases with the mass filling rate. The final gas temperature values depend further on the ambient temperature, the inlet gas temperature and the initial tank pressure (initial SOC). It has also been demonstrated experimentally that the gas temperature distribution is not uniform inside the tank during the filling; in general the gas temperature increases with the distance from the inlet, with a possible hot spot at the upper part of the rear dome and is lower than average temperature very near the gas jet inlet. The spatial temperature difference tends to increase with the dimensions and the aspect length-to-diameter ratio of the tanks. Also the gas jet nozzle diameter can cause and can influence local temperature differences. It has been reported that a hot spot created in the upper area of the tank tends to decrease with the decrease of the jet nozzle diameter [20].

In most of the filling experiments and simulations it is assumed that the tank temperature at the beginning of filling is the same as ambient temperature. There are not many studies about the thermal behaviour of hydrogen tanks during emptying and about the fast filling of tanks starting from non-equilibrium conditions, which could be also a reality in a refuelling station. Y. Matsuno et al. [21] studied the influence of the test starting conditions in a sequence of hydrogen cycles in Type III and Type IV tanks. Results indicated that although in the first 3 to 4 cycles of the cycling sequence the attained temperatures were varying, they became stable after that; when the heat transfer between the tank, the filling gas and the gas in the tank reached equilibrium. So, they concluded that the test starting conditions had little influence on the attained temperature of the gas in the tank during the long term cycling.

There is no specification for the location of temperature measurement points on on-board tanks. For research purposes, different configurations have been designed to instrument the tanks with different thermocouples inside [4, 17]. These configurations are not practical for a qualification of design of a tank or even in a refueling station. Therefore, some tanks are equipped with an integrated control system including one thermocouple placed inside the tank very near the nozzle. In the hydrogen gas cycling test defined in the ISO/TS 15869: 2009 standard [8], it is specified that temperature shall be monitored using thermocouples attached to the metal end boss at both ends of the fuel tank. It is also mentioned that care should be taken to ensure that temperatures during filling and venting do not exceed the specified service conditions. However, the service conditions only define the maximum

and minimum hydrogen temperature inside the tank and nothing is mentioned about the temperature of the bosses. The monitoring of the tanks external temperatures (bosses and outer walls) during hydrogen cycling tests to estimate the inside gas temperature is still an open field of research.

In this study, a detailed analysis of the operational conditions during the hydrogen cycling of three different commercial (Type III and Type IV) tanks has been done. The temperature of the gas at different points inside the tanks and the outside temperatures (at the bosses and the tanks outer walls) have been also evaluated and compared during the cycles.

## 2. EXPERIMENTAL

### 2.1 Description of the characteristics and the instrumentation of the tanks

Three different hydrogen storage different tanks with the same 70 MPa NWP have been used in this study. In Tab. 1, the characteristics of the tanks are given.

Table1: Characteristics of the tested type IV and type III cylinder tanks

	Type IV 19L	Type IV 28.9L	Type III 40L
<b>Materials</b>			
Liner	HDPE	HDPE	AA
End Bosses	AA	SS	AA
Composite shell	CFRE	G&CFRE	CFRE
<b>Vessel Mass (Kg)</b>	18.3	32.9	41.5
<b>Storage Volume (L)</b> (at 70 MPa)			
	19	28.9	40
<b>H<sub>2</sub> capacity (Kg)</b> (with fill density of 40.22 Kg/m <sup>3</sup> )			
	0.76	1.16	1.60
<b>Unpressurized dimensions (mm)</b>			
External length	904	827	920
External diameter	228	279	329
Internal diameter	180	230	290

HDPE: High density polyethylene, CFRE: Carbon fiber-reinforced Epoxy, G&CFRE: Glass and carbon fibre reinforced Epoxy, AA: Aluminium Alloy, SS: Stainless Steel

Each tank has been instrumented with 8 thermocouples (TC) and with resistance temperature detectors (RTD). As depicted in Fig. 1, the TCs (labeled from 1 to 8) measure the temperature of the gas at different positions. One TC was inserted through the gas inlet opening and the other seven by means of a special tree-shape array introduced from the rear of the tank. The RTDs (labeled  $T_{Front}$ ,  $T_{Rear}$ ,  $T_{Top}$  and  $T_{Bottom}$ ,) were placed on the outside of the tank to measure the temperature of the bosses and the tanks walls (in the cylindrical part at the same distance as the central TCs).

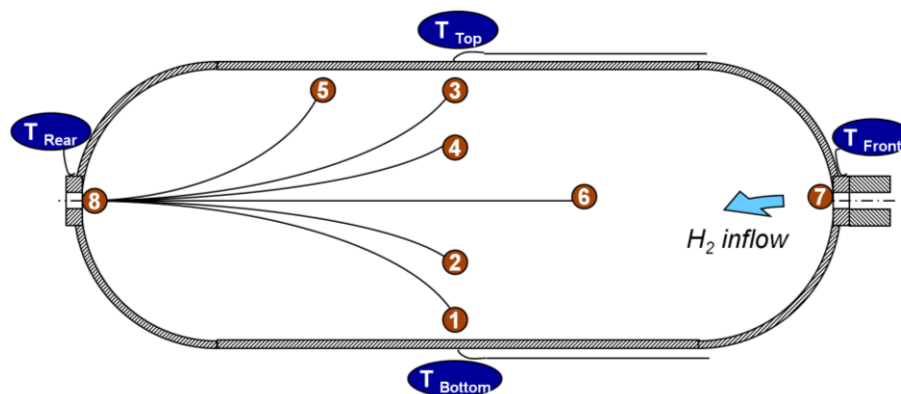


Figure 1. Arrangement of the temperature measurement instrumentation in the tested tanks

In Tab. 2, the exact position of the thermocouples inside each tank is given as the distance from the central axis and from the rear boss respectively. Regarding the outside temperatures, in Tab. 2 the temperatures that were measured are indicated by an x.

Table 2: Position of the thermocouples (linear distance from the cylinder's central axis and from the Rear Boss respectively) and description of the measured outside temperatures in the different tanks.

	Position of the TCs (mm)								Outside Temperatures			
	TC1	TC2	TC3	TC4	TC5	TC6	TC7	TC8	T <sub>Front</sub>	T <sub>Rear</sub>	T <sub>Top</sub>	T <sub>Bottom</sub>
Type IV 19L	-87 340	-43 305	88 345	42 300	90 255	0 308	0 843	0 65	x	x	-	-
Type IV 28.9L	-110 240	-55 225	107 245	55 225	115 160	0 248	0 767	0 65	x	-	-	x
Type III 40L	-95 555	-65 527	95 550	67 533	145 292	0 560	0 855	0 65	x	x	x	x

The used thermocouples were 1mm thick type K, capable to measure temperatures between -200°C to 1250°C with an uncertainty of 2.2°C. The thermocouples system was calibrated for the expected gas temperature range inside the tanks (from -50°C to 100°C). The RTDs used had a nominal resistance of 100 Ohms at 0°C and were capable to measure temperatures in a range of -100°C to 550°C with a maximum deviation of 1.25°C. The tanks' gas pressure was measured using a pressure transducer placed at the rear of the tank. The pressure transducers were calibrated for high pressure range (the measurement error is 5% for pressures lower than 10 MPa and 0.64% at 70 MPa). In all cases a gas jet nozzle of 3 mm diameter has been used.

## 2.2 Description of the Fast Filling tests

### 2.2.1 Description of the GasTeF facility

The tanks have been hydrogen cycled in the GasTeF facility of the Joint Research Centre of the EC [22]. Each tank is placed in a closed sleeve with 380 L inner volume maintained under a continuous flow of nitrogen (of 350-500 Nml/min). Thermocouples are placed in the sleeve and in the gas distribution lines to monitor the tank environmental temperature and the filling gas temperature during the tests. These temperatures vary only negligible during the cycling campaigns. GasTeF facility is fully automated and tests are supervised remotely from a control room. All the facility operational data and the measurements from the scientific instrumentation are automatically recorded by the control system. The time interval for data logging is 0.6 seconds.

The filling of the tanks is performed in two stages. The first stage consists in a pressure equilibration process between an external hydrogen reservoir and the tank to be tested. The reservoir has a capacity of 1800 L and is kept at a pressure of 20 -25 MPa. When the pressure of the tank is equilibrated with the one in the gas reservoir, the second filling stage starts; the compressor pumps the gas, filling the tank to the required final pressure and at the required speed. The same two stages occur also during the emptying of the tanks. The combination of the two stages results generally in a non-linear pressure rise profile. The value of the pressure filling rate and mass flow rate given in this paper represent an average value calculated considering the total time required for reaching the final pressure. They will be called Average Pressure Ramp Rate (APRR) and Average Mass Ramp Rate (AMRR) respectively.

### 2.2.2 Description of the tests and the controlled operating conditions

The Type IV 19L tank was sequentially hydrogen cycled during a fatigue test campaign that lasted about two months. The filling rate was varying along the campaign. For this paper, 40 cycles have been analysed. The hydrogen cycles consisted in a filling of the tank from 3.0 to 84.0 MPa with duration ranging from 5 to 8 minutes, a 16 minutes holding time and a slow emptying of the tank back to 3.0 MPa for 35 ± 3minutes.

In the Type IV 28.9L tank, 10 sequential hydrogen cycles were performed. In this case, the cycling parameters were kept constant; the tank was filled from 2.0 to 77.5 MPa in about 4 minutes, then, it was kept under the high pressure during 2 to 3 minutes and finally, it was slowly emptied back to 2.0 MPa in  $50 \pm 3$  minutes.

In the Type III 40L tank, 10 sequential hydrogen cycles were performed. The cycling parameters were the same as for the Type IV 28.9L tank with the exception of the filling and emptying times, which have been changed parametrically. The tank has been filled from 2.0 to 78.5 MPa with a filling time ranging from 3 to 10 minutes, then it has been kept under high pressure during 2 to 3 minutes and finally it has been slowly emptied back to 2.0 MPa with an emptying time ranging from 34 to 52 minutes.

For the performed cycles and for each start and end of the filling, holding and emptying phases, the following parameters have been calculated:

1. A tank-averaged gas temperature  $T_{Av}$  (defined as the average of 5 temperatures measured from Top to Bottom in the tanks, TC5, TC4, TC6, TC2 and TC1; assuming homogeneous gas density during filling, the value can be considered a mass-averaged temperature).
2. The spatial difference between the maximum and minimum gas temperatures measured by the TCs (TC1 to TC8) inside the tank at each phase; e.g. at the end of the filling phase:  $\Delta TC = TC_{Max}(\text{end of filling}) - TC_{Min}(\text{end of filling})$ .
3. The difference between final and initial average temperatures in each phase; e.g. during the filling phase:  $\Delta T_{Av} = T_{Av}(\text{end of filling}) - T_{Av}(\text{start of filling}) = T_{FAv} - T_{0Av}$ .

The average mass ramp rates during filling and emptying and the state of charge (1) of the tanks after filling and after emptying were also calculated for the performed cycles.

For the mass calculation, the Redlich-Kwong equation of state (2), widely used in chemical and petroleum industries and able to predict accurately hydrogen properties in a wide range of temperature and pressures, has been used. This equation relates pressure  $P$  (in kPa), temperature  $T$  (in degrees Kelvin) and molar volume  $v$  (in L/mole) using the gas constant  $R$  ( $8.314 \text{ L}\cdot\text{kPa}\cdot\text{K}^{-1}\cdot\text{mol}^{-1}$ ) and two coefficients ( $a$  and  $b$ ) which depend on the critical temperature and pressure of the gas used [23].

$$P = \left( \frac{R \cdot T}{v - b} \right) - \frac{a}{v \cdot (v + b) \cdot \sqrt{T}}, \quad (2)$$

### 3. RESULTS AND DISCUSSION

#### 3.1 Experimental conditions and results

In Tab. 3, a summary of the different conditions used and the results obtained is shown.

Fig. 2 shows the time dependences of pressure and gas temperatures of the three tested tanks during a hydrogen cycle. The values of thermocouples TC1 to TC6 are given as representative of the average tank gas temperature. The values of TC7 and TC8 are not shown because they are strongly influenced by the bosses.

Table 3. Characteristics of the cycles performed in different type IV and type III cylinder tanks

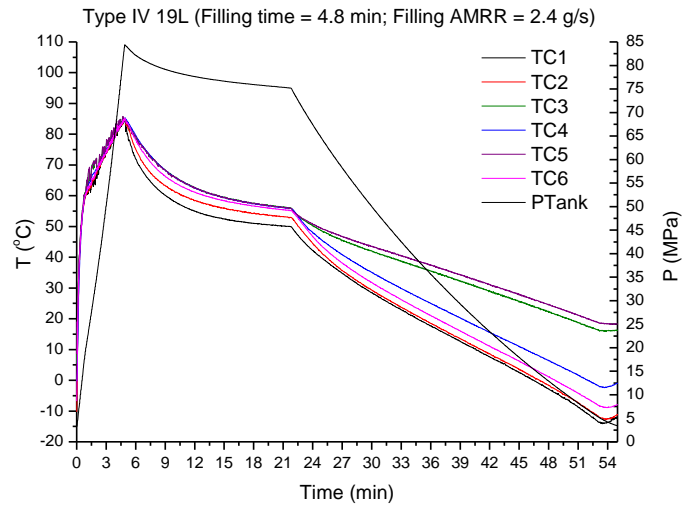
	Type IV 19 L	Type IV 28.9L	Type III 40 L
<b>Number of cycles</b>	40	10	10
<b>Ambient T (°C)</b>	25-30	16-21	17-20
<b>Filling gas T (°C)</b>	27-32	22-25	23-26
<b>P (MPa)</b>			
Low P	3.0– 3.4	1.9 – 2.0	1.9 – 2.0
High P	83.7 – 84.6	77.0 – 78.2	77.9 – 79.1
P after holding	73.9 – 79.5	73.0 – 73.8	75.1 – 76.8
<b>Time (min)</b>			
Filling time	4.8 – 8.1	4.2 – 4.3	2.6–9.7
Holding time	15.3 – 17.7	2.0 – 3.0	2.0 – 3.0
Emptying time	31.6 – 37.8	47.4 – 51.5	33.6 – 51.5
<b>T<sub>Av</sub> (°C)</b>			
End emptying	-8.2 – 5.5	-12.5 – 0.2	-1.3 – 4.0
End Filling	70.7 – 85.5	83.4 – 91.0	81.2 – 64.0
End Holding	49.1 – 58.2	65.5 – 74.7	66.5 – 57.1
<b>ΔTC (°C)</b>			
End emptying	23.4 – 30.3	24.4 – 27.7	8.3 – 14.4
End Filling	0.1 – 3.2	0.5 – 1.7	0.6 – 2.8
End Holding	4.7 – 7.8	14.4 – 15.9	3.8 – 6.1
<b>ΔT<sub>Av</sub> (°C)</b>			
Filling	78.9 – 87.4	90.8 – 95.8	64.5 – 77.1
Holding	-32.4 – -21.1	-18.3 – -13.9	-6.0 – -14.7
Emptying	-58.3 – -53.1	-79.7 – -72.6	-46.1 – -64.0
<b>AMRR (g/s)</b>			
Filling	1.4 – 2.3	3.8 – 4.0	2.5 – 9.2
Emptying	0.33 – 0.38	0.32 – 0.35	0.46 – 1.1
<b>SOC (%)</b>			
Empty	6.7 – 7.4	4.3 – 4.4	4.1–4.4
Full	95.2 – 97.8	89.2 – 90.2	92.1 – 94.8

It must be noted that the initial gas temperature distribution inside the tank is not homogeneous. This is due to the fact that experiments shown here consist of a series of filling-emptying cycles performed sequentially, so that after an emptying phase, which causes a non-uniform gas temperature distribution, a new filling phase starts.

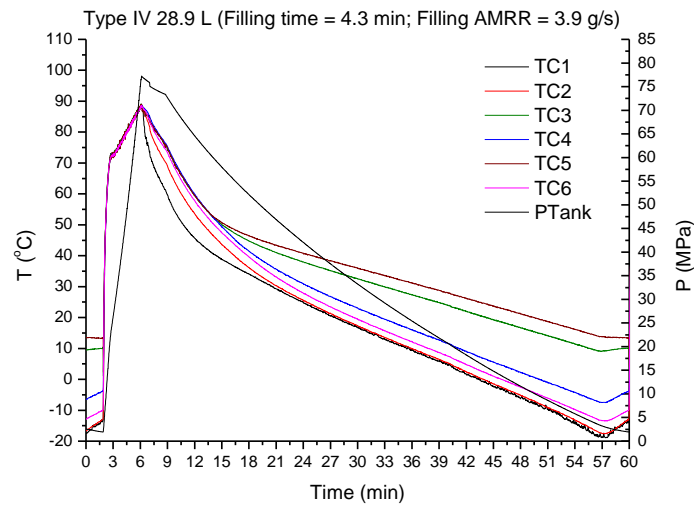
Despite the different initial values, all the 1 to 6 positions show the same value immediately from filling start. During the whole filling duration the gas temperature distribution is very uniform for all the tanks tested. This can be explained on one side by forced convection induced by the gas injection [20], and on the other side by the relative small volumes of the tanks tested.

As expected, the maximum temperatures reached at the end of the filling were higher in the Type IV than in the Type III tank. In the Type IV 19L tank, lowering the filling time down to 4.8 minutes (corresponding to a mass flow rate of 2.4 g/s and to a SOC moving from 7% of 95%), the temperature limit of 85°C was reached. In the Type IV 28.9L tank, and with a filling of about 4.2 minutes (corresponding to a mass flow rate of about 3.9 g/s and to a SOC from 4% to 90%), nearly in all cases, the 85°C limit was exceeded. On the contrary, in Type III 40L tank and filling the tank as fast as in 2.6 minutes (9.2 g/s), from a SOC of about 4% to 92%, the maximum temperature reached was 81°C.

a



b



c

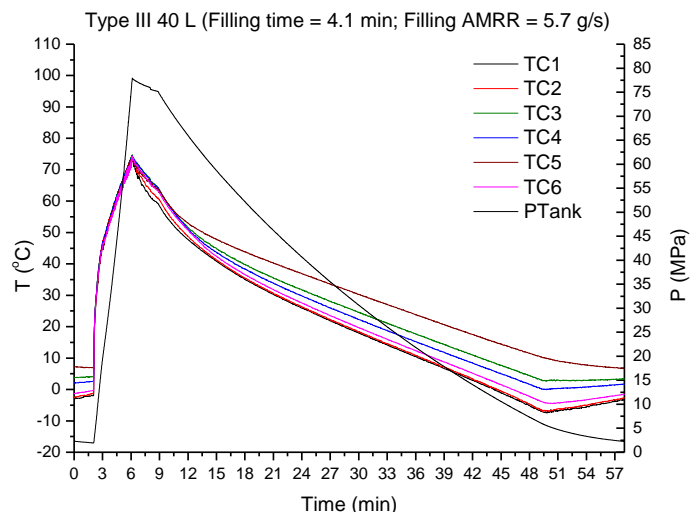


Figure 2. Pressure and inside temperature (TC1 to TC6) profiles during a hydrogen cycle with similar filling times (between 4 and 5 minutes) and Emptying AMRR (between 0.3 and 0.5 g/s); (a) Type IV 19 L tank (b) Type IV 28.9L tank and (c) Type III 40 L tank.

After filling, during holding and emptying the tanks, a vertical gas temperature gradient occurs, causing  $TC5 > TC3 > TC4 > TC6 > TC2 > TC1$ . This phenomenon is caused by gas buoyancy induced by gas density differences [17], and is more significant in Type IV tanks than in Type III. In the course of the emptying, the temperature distribution in the bottom third of the tanks tends to homogenize as indicated by TC1 and TC2 values that become almost identical. For Type IV tanks, the buoyancy effect results in a top-bottom temperature difference ranging between 23°C and 30°C at the end of the emptying phase (with an emptying rate of 0.34 g/s). The vertical temperature gradient is not linear, with the highest temperature difference occurring in the upper third of the tank, between TC4 and TC5.

In the case of the Type III tanks, for the emptying rates used, between 0.46 g/s and 1.10 g/s, the top-bottom difference ranged only between 8°C and 14°C. The vertical gradients in this case results more linear than in type IV tanks. It was also observed that, the faster the emptying, the higher was the stratification of the gas temperature distribution.

### **3.2 Thermal behaviour of the gas**

#### **3.2.1 Effect of filling mass flow rate**

In Fig. 3, the gas average temperature rise during the filling phase  $\Delta T$  is plotted as function of the mass flow rate. The data shown are not perfectly comparable because affected by slightly different initial gas temperature values. To simplify analysis and interpretation, the  $T_{0\text{Av}}$  has been indicated in the legend of the figure. Two points have also been singled out for the Type III tank. They correspond to an equilibrium case, with perfectly homogeneous gas temperature distribution before filling that cannot be compared with the others. Their initial temperatures of 8.7°C and 18.2°C, called  $T_{0\text{Eq}}$  in the figure, result also higher than those of the other data, ranging between -1.3°C and 7.2°C.

In all cases, as expected, the temperature rise increases with the mass flow rate. Due to the higher thermal conductivity of the aluminium alloy liner, for comparable filling rates, the temperature rise in Type IV tanks is higher than in Type III tank. It can be also observed that the higher the filling rate, the higher results the difference of temperature rise between Type IV and Type III tank.

#### **3.2.2 Effect of initial temperature.**

In the insert in the upper right corner of Fig. 3,  $\Delta T_{\text{Av}}$  is plotted as function of the starting gas average temperature  $T_{0\text{Av}}$  for different fillings in Type IV tanks performed with the same mass flow rates (2.0 g/s for the Type IV 19L tank and 3.9 g/s for the Type IV 28.9L tank). Under these conditions it appears that the rise in gas temperature during the filling tends to decrease with the initial temperature of the gas.

A possible explanation is linked to the fact that higher initial gas temperatures cause a higher heat exchange with the environment. The temperature range available in this data set is however not enough to allow general conclusion.

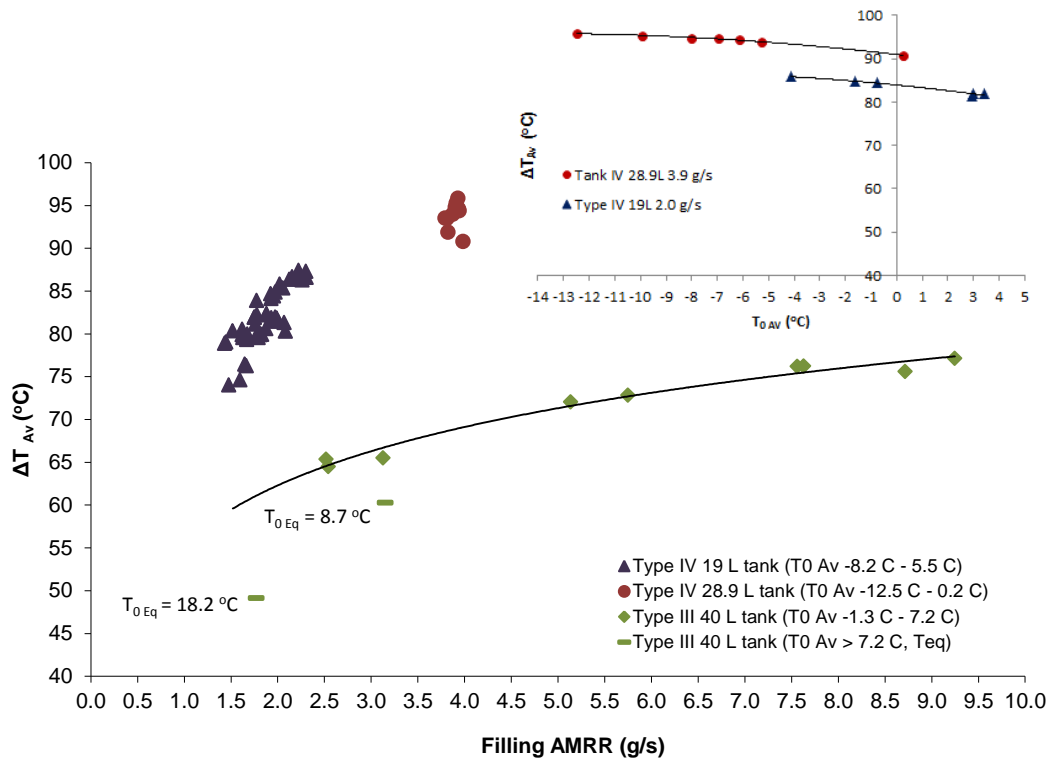


Figure 3. Effect of filling rate and tanks initial temperature on the gas average temperature increase during the filling of Type IV 19L, Type IV 28.9L and Type III 40 L tanks. The lines are guide for the eye.

### 3.3 Thermal behaviour of the external surface of the tanks during the cycles.

In this section the external temperatures of the tank are analysed and related to the internal gas temperature evolution. Fig. 4 shows the internal and external thermal behaviour during a hydrogen cycle for each of the three tanks tested: (a) Type IV 19 L, (b) Type IV 28.9L and (c) Type III 40 L. The graphs at the left hand side of Fig. 4 show all the external surface temperatures available (Table 2) and compare them with the average gas temperature inside the tank ( $T_{av}$ ) for the whole filling-emptying cycle. On the right hand side, the graphs show bosses and average gas temperatures and pressure in the first five minutes of the cycle to investigate a possible internal and external temperature correlation during the filling phase.

#### 3.3.1 Thermal response of the tanks top and bottom walls

As mentioned in the previous section, the hydrogen cycles are performed sequentially and the filling phase starts with a non-uniform temperature distribution of the gas in the tank, caused by the previous emptying phase. It has been also observed that there is a linear correlation between the internal and external temperatures at the end of the emptying phase. In Type IV 28.9L tank and for the emptying rate of 0.34 g/s, the tanks bottom wall was 15.8°C warmer than the inside gas. In Type III 40 L tank, due to the higher thermal conductivity of the aluminium alloy liner (compared to the polyethylene one), this gradient was smaller. For the slowest of the filling rates used (0.46 g/s), the Bottom and the Top walls were respectively, 5.2°C and 9.4°C warmer than average gas temperature. For a faster emptying rate (0.71 g/s), the temperature gradients were bigger, 11.8°C and 19.0°C respectively. From the given data for Type III tanks it can be observed that after the emptying, the Top wall is warmer than the Bottom wall, difference that is even higher the faster is the emptying rate. In Type IV tanks, due to the observed higher stratification of the gas temperature inside the tanks during the emptying, the temperature difference between the walls is expected to be even higher.

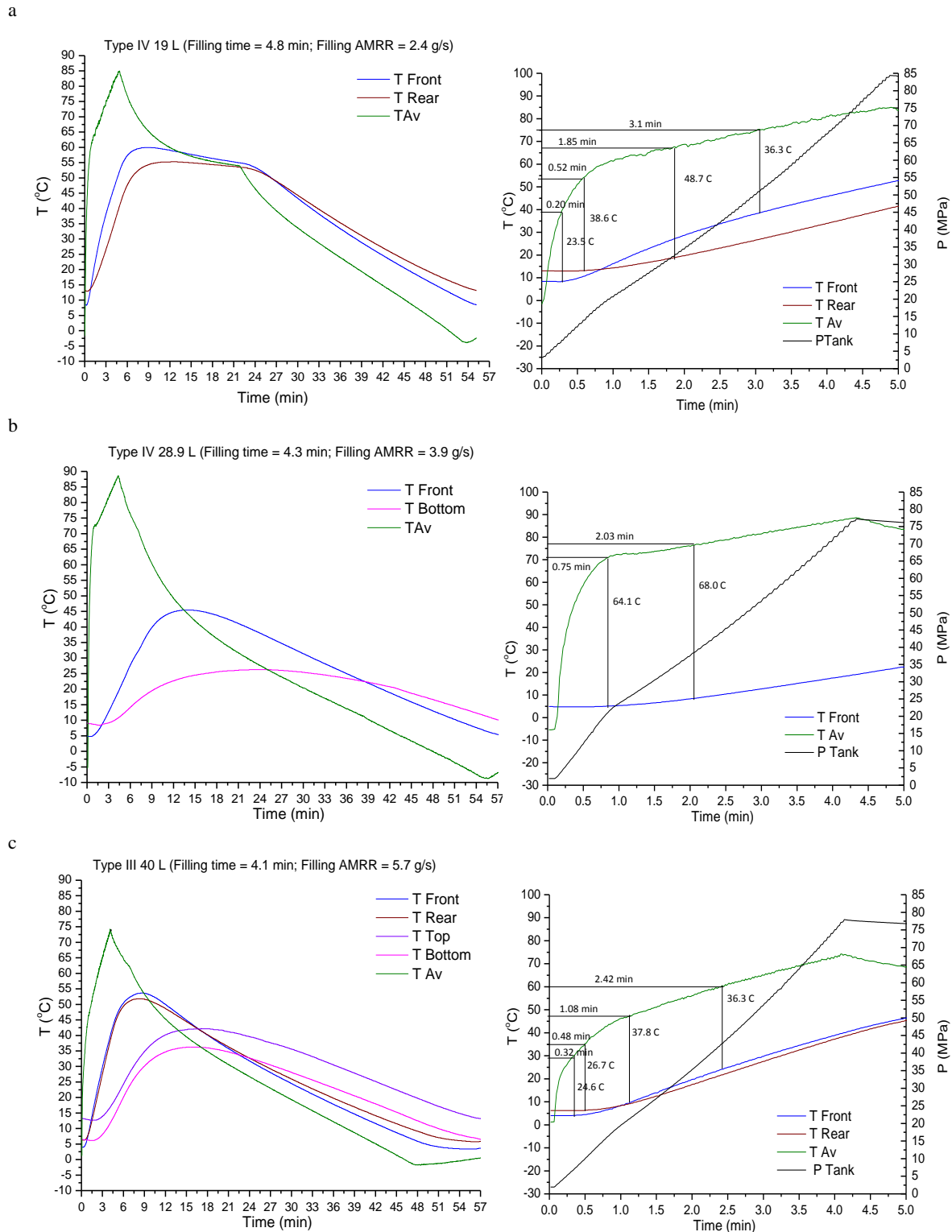


Figure 4. Evolution of the external tanks temperatures ( $T_{Front}$ ,  $T_{Rear}$ ,  $T_{Top}$  and  $T_{Bottom}$ ) and the average gas temperature during a hydrogen cycle with similar filling times (between 4 and 5 minutes) and emptying rates (between 0.3 and 0.5 g/s); (a) Type IV 19 L tank (b) Type IV 28.9L tank and (c) Type III 40 L tank.

The different thermal conductivity and the different time-dependent heat transfer of the two types of tanks trigger clear differences in the evolution of the bottom wall temperature. As shown in Fig. 4, at the end of the filling phase  $T_{Bottom}$  of Type III tank shows a temperature increase of 41% of the average gas temperature, while relative increase of  $T_{Bottom}$  is only 18% for Type IV tank. Moreover,

$T_{\text{Bottom}}$  reaches its maximal value 10.9 minutes after the end of the filling phase in the Type III tank and only after 18.7 minutes for Type IV tank.

Only for the Type III tank both  $T_{\text{Top}}$  and  $T_{\text{Bottom}}$  have been recorded. Along the whole filling-emptying cycle the two temperatures show an almost constant difference, except in the last part of the filling phase, when their difference reduces. This can be explained considering the internal gas temperature. At the beginning of the filling phase, the difference between  $T_{\text{Top}}$  and  $T_{\text{Bottom}}$  derives from the horizontal stratification of the gas temperatures occurring during the previous emptying phase. As seen above in 3.1, during filling the internal temperature is perfectly homogenised. Consequently, with a certain delay, also the external wall surface temperatures tend to converge. However, as soon as the emptying phase starts, the internal stratification makes the external temperatures to assume their original different values.

It can be thus concluded that the outer walls of the tanks follow the inside gas temperature during the hydrogen cycling. The control of the outer walls temperatures can give an idea of the stratification and the thermal exchange of a tank during hydrogen cycling. However, due to the big inertia of the walls, it is very difficult to follow the evolution of the inside gas temperature during a fast filling monitoring only these external temperatures.

### 3.3.2 Correlation between tank internal and external temperatures

Comparing the front boss temperature evolution of the three different tanks during the hydrogen cycle shown in Fig. 4, it can be seen that  $T_{\text{Front}}$  reaches its maximal value much earlier in Type III 40L and Type IV 19 L tanks than in Type IV 28.9 L tank. This is due to the higher thermal conductivity of the aluminium alloy compared to the stainless steel, causing a quicker and higher heat transfer through the boss thickness. The aluminium alloy boss in Type IV tank experiences a temperature which is 59 % of the gas one during the filling. Its maximal temperature is reached 3.5 minutes after the filling phase is finished. In the case of the stainless steel boss of Type IV tank, its external temperature is only 43% of the gas one and its maximum is reached later, 8.5 minutes after end of the filling phase.

Comparing the Front and Rear bosses in Type IV 19L and in Type III 40L tanks, it can be observed that during the hydrogen cycles shown, especially in the Type IV tank, the front boss follows more closely the inside gas temperature than the rear boss.

The graphs at the right hand side of Fig. 4 show the temperatures of the external boss surfaces during the filling phase,  $T_{\text{Front}}$  and  $T_{\text{Rear}}$ . Their response time, defined as the time at which  $T_{\text{Front}}$  or  $T_{\text{Rear}}$  shows a first increase, are quantitatively indicated in the graphs, as well as the moment when they start to show a linear dependence on filling time. The differences between  $T_{\text{Front}}$  or  $T_{\text{Rear}}$  and the tank internal gas temperature are also given.

It can be observed that due to the big thermal inertia of the stainless steel boss in Type IV 28.9 L tank, the front boss only started warming when there was already a temperature difference of 64°C with the inside gas temperature.

It can be also observed that the front bosses had a faster response than the rear bosses. However, the rear bosses' temperature started to be linear earlier than the front bosses' temperature (which is influenced by the gas inlet flow). This observation suggests that it may be easier to find a correlation of the inside gas temperature with the rear bosses than with the front bosses.

In Fig. 5, the average gas temperature has been plotted against (a)  $T_{\text{Front}}$  and (b)  $T_{\text{Rear}}$  for different mass flow rates and different tanks. The linear part of each curve has been identified by a linear regression ( $R \approx 0.997$ ) and has been marked as a thicker line.

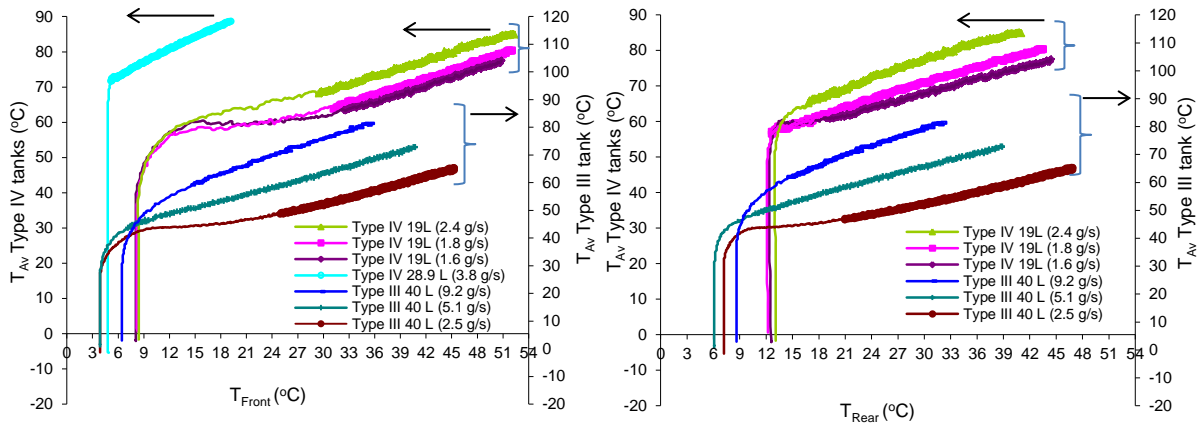


Figure 5. Correlation between tank average gas temperature  $T_{Av}$  and the temperature of (a) the front bosses  $T_{Front}$  and (b) the rear bosses  $T_{Rear}$  during the filling phase. Each curve represents one mass flow rate. Gas temperatures of Type IV tanks are given on the left y-axis while those of Type III tanks are plotted on the right y axis, for each of the two graphs. The thicker parts of each curve indicate the linear behaviour of  $T_{Front}$  and  $T_{Rear}$ .

In this data representation, the case of the Type IV 28.9L tank with stainless steel bosses stands out clearly as an outlier. In the case of the Type IV 19L tank with aluminium bosses,  $T_{Rear}$  become linear earlier than  $T_{Front}$ . The same trend is visible in Type III tank, but to a less extent.

In the case of the Type III tank, higher mass flow rate caused higher final gas temperature but lower bosses temperatures (the lower was the heat transfer of the gas with the bosses). This difference was more pronounced in the rear bosses. In the Type IV tank this effect is not observed. However, the range of mass flow rate investigated in this study with Type IV tanks is much smaller than in that explored in Type III tank, so that this comparison is not enough to draw general conclusions.

#### 4. CONCLUSIONS

The thermal behaviour of hydrogen tanks of type III and IV has been studied under refuelling and emptying conditions. Particular attention has been dedicated to local temperature measurements of the gas inside the tank as well as of the external surface of the tanks. Their time-dependent behaviour has been analysed and compared. All tests have been performed without pre-cooling.

During the hydrogen filling phase, the temperature distribution of the gas inside the tank is almost uniform. On the contrary, during the holding and the emptying phases, stratification in the gas temperature is significant in both type tanks, being much higher in Type IV tanks (where big temperature gradients appear in the upper third of the tank). The faster the emptying, the higher was the stratification of the gas temperature.

The gas average temperature towards the end of the emptying phase is proportional to the tanks' walls temperatures, and local external temperatures react to the local internal temperature distribution. The top surface of the tank is always warmer than the bottom surface. The faster the emptying rate, the higher were the gradients (between the inside gas and the walls) and the higher the difference between bottom and top walls.

During hydrogen filling, the temperature increase in Type IV tanks was higher than in Type III tanks. The higher is the filling mass flow rate, the bigger is the difference between the final temperatures of Type III and Type IV. Under comparable conditions, the maximum temperature at the end of the filling phase is lower in Type III than in Type IV tank. In Type III tank, more than twice faster fillings

have been possible without reaching the allowable maximum temperature limit of 85 °C. The higher the initial temperature of the tanks, the lower is the rise of the gas temperature. This can be associated to higher heat losses to the environment at higher tank temperatures.

The external surface temperatures follow the internal thermal evolution with a time delay which depends on the measurement position, the tank type and the materials, as well as on the mass flow rate used during filling and emptying. As expected, the difference between the inside gas temperature and the tanks walls is bigger in Type IV than in Type III tanks.

Therefore, and to a certain extent, external surface temperatures could give information on gas temperature distribution during hydrogen cycling. However, due to the big thermal inertia of the walls, it will be very difficult to control maximal temperature evolution of the hydrogen and the internal tank surfaces during a fast filling, by monitoring only these external temperatures.

To this respect, an aluminium alloy boss is to be preferred to a stainless steel one, because the external temperature of the former is closer than the latter to that of the gas. Moreover, the front boss follows more closely the inside gas temperature than the rear boss. On the contrary, during the filling phase, the external temperature starts to be linear earlier at the rear than at the front boss. This observation suggests that it could be easier to find a correlation between the rear boss and the average gas temperature. To allow this, however, more experimental data are still needed.

## REFERENCES

1. M. Klell, M. Zuschrott, H. Kindermann, M. Rebernik, Thermodynamics of hydrogen storage, 1st International Symposium on Hydrogen Internal Combustion Engines, 2006, Graz-Austria.
2. L. Zhou, Progress and problems in hydrogen storage methods, *Renewable & Sustainable Energy Reviews*, **9**, 2005, pp. 395-408.
3. Hydrogen production and storage, International Energy Agency (IEA), 2006, Paris-France.
4. B. Acosta, P. Moretto, N. Frischauf, F. Harskamp, C. Bonato, ICHS 2011, San Francisco-California.
5. S. C. Kim, S. H. Lee, K. B. Yoon, Thermal characteristics during hydrogen fueling process of type IV cylinder, *International Journal of Hydrogen Energy*, **35**, 2010, pp. 6830-6835.
6. Regulation (EC) No 79/2009 of the European Parliament and of the Council of 14 January 2009 on type-approval of hydrogen-powered motor vehicles, and amending directive 2007/46/EC.
7. SAE J2579 Technical Information Report for Fuel Systems in Fuel Cell and other Hydrogen Vehicles, 2008, SAE International.
8. ISO/CD 15869-Gaseous hydrogen and hydrogen blends – Land vehicle fuel tanks, ISO 2008.
9. SAE J2601, Fuelling Protocols for Light Duty Gaseous Hydrogen Surface Vehicles, Issue 2010, SAE International.
10. M. Xi, P. Xiangmin, L. Zhiyong, M. Jianxin, Research progress of fast filling of high pressure hydrogen for fuel cell vehicles, ICEICE 2011, Wuhan, China.
11. S. Pregassame, F. Barth, L. Aullidieres, K. Barral, Hydrogen refuelling station: filling control protocols development, WHEC 2006, Lyon, France.
12. C. Powars, S. Unnasch, E. Kassoy, S. Venkatesh, J. Williams et. al., California Hydrogen Fuelling Station Guidelines, 2004, TR-03-163a TIAX Case D0228.
13. Y.L. Liu, Y.Z. Zhao, L. Zhao, X. Li, H.G. Chen, L.F. Zhang, H. Zhao, R.H. Sheng, T. Xie, D.H. Hu, J.Y. Zheng, Experimental studies on temperature rise within a hydrogen cylinder during refuelling, *International Journal of Hydrogen Energy*, **35**, 2010, pp. 2627-2632.
14. L. Zhao, Y. Liu, J. Yang, Y. Zhao, J. Zheng, H. Bie, X. Liu, Numerical simulation of temperature rise within hydrogen vehicle cylinder during refuelling, *International Journal of Hydrogen Energy*, **35**, No. 15, 2010, pp. 8092-8100.

15. W. E. Liss, M. E. Richards, K. Kountz, K. Kriha, Modelling and Testing of Fast-Fill Control Algorithms for Hydrogen Fuelling, National Hydrogen Association Meeting, 2003, Washington DC.
16. M. Heitsch, D. Baraldi, P. Moretto, Numerical investigations on the fast filling of hydrogen tanks, *International Journal of Hydrogen Energy*, **36**, No. 3, 2011, pp. 2606-2612.
17. C. J. B. Dicken and W. Merida, Measured effects of filling time and initial mass on the temperature distribution within a hydrogen cylinder during refuelling, *Journal of Power Sources*, **165**, 2007, pp. 324-336.
18. C. J. B. Dicken and W. Merida, Modeling the transient temperature distribution within a hydrogen cylinder during refuelling, *Numerical Heat Transfer; Part A: Applications*, **53**, 2008, pp. 685-708.
19. S. Pregassame, F. Michel, L. Allidieres, F. Bourgeois, K. Barral., Evaluation Of Cold Filling Processes For 70MPa Storage Systems In Vehicles, WHEC 2006, Lyon-France.
20. T. Terada, H. Yoshimura, Y. Tamura, H. Mitsuishi, S. Watanabe, Thermal Behavior in Hydrogen Storage Tank for FCV on Fast Filling (2nd Report), SAE Technical Paper doi:10.4271/2008-01-0463, 2008.
21. Y. Matsuno, Y. Maeda, N. Otsuka, Y. Tamura, H. Mitsuishi, Attained temperature during gas fueling and defueling cycles of compressed hydrogen tanks for FCV, ICHS 2011, San Francisco California.
22. B. Acosta, P. Moretto, N. Frischauf, F. Harskamp, C. Bonato, GASTEF: The JRC-IE Compressed Hydrogen Gas Tanks Testing Facility, WHEC 2010, Essen-Germany.
23. K. Nasrifar, Comparative study of eleven equations of state in predicting the thermodynamic properties of hydrogen, *International Journal of Hydrogen Energy*, **35**, 2010, pp. 3802-3811.